H. S. Tzou
Y. Bao
Department of Mechanical Engineering
Center For Robotics and Manufacturing Systems
University of Kentucky
Lexington, KY 40506-0046

Dynamics and Control of Adaptive Shells with Curvature Transformations

Adaptive structures with controllable geometries and shapes are rather useful in many engineering applications, such as adaptive wings, variable focus mirrors, adaptive machines, micro-electromechanical systems, etc. Dynamics and feedback control effectiveness of adaptive shells whose curvatures are actively controlled and continuously changed are evaluated. An adaptive piezoelectric laminated cylindrical shell composite with continuous curvature changes is studied, and its natural frequencies and controlled damping ratios are evaluated. The curvature change of the adaptive shell starts from an open shallow shell (30°) and ends with a deep cylindrical shell (360°). Dynamic characteristics and control effectiveness (via the proportional velocity feedback) of this series of shells are investigated and compared at every 30° curvature change. Analytical solutions suggest that the lower modes are sensitive to curvature changes and the higher modes are relatively insensitive. © *1995 John Wiley & Sons, Inc.*

INTRODUCTION

The concept of adaptive geometry dates back to the early years of robotics and adaptive truss structures (Paul, 1981; Natori, Iwasaki, and Kuwao, 1987; Miura and Furuya, 1988; Wada, Fanson, and Crawley, 1989). Adaptive structural systems with inherent active adaptation and geometry transformation are very attractive in many applications, for example robotics, airplanes, vehicles, marine (surface or underwater) ships, micromechanical systems, etc. With the development of active electromechanical materials and actuators, this geometry adaptation is a step closer to reality. This article is concerned with an evaluation of control effects of a piezoelectric laminated cylindrical shell composite with a total of 330° curvature change. Possible applications of the configuration are compressors and fan shrouds for active blade tip clearance control, and reflectors with active dynamics and radius control, etc. Dynamics and active control effects of these transforming shells with different curvatures are studied and compared. Mathematical modeling of the piezoelectric laminated cylindrical shell is presented first, followed by analytical solution procedures and case studies.

PIEZOELECTRIC CYLINDRICAL SHELL COMPOSITE SYSTEMS

A cylindrical shell is defined in a cylindrical coordinate system: x, θ, and α_3, in which x defines the length (longitudinal) direction, θ the circumferential direction, and α_3 the transverse direction. It

Received August 25, 1994; Accepted October 16, 1994
Shock and Vibration, Vol. 2, No. 2, pp. 143–154 (1995)

CCC 1070-9622/95/020143-12

is assumed that the curvature change is induced by strong external actuation forces, and a series of cylindrical shells with different curvatures are then created. Dynamics and control of these shells with different curvatures are assumed linear and evaluated at small vibration amplitudes with respect to their static equilibrium position. Accordingly, the externally applied actuation forces causing the curvature changes are not considered in the analysis. Electromechanical equations at each deformed state of static equilibrium can be defined by its curvature angle and accordingly its dynamics and control can be evaluated. Control effect is introduced by the piezoelectric actuator, layers, via the converse piezoelectric effect, at its deformed equilibrium position (Tzou, 1993). Figure 1 illustrates the shell transformation process from an open cylindrical shell panel to a deep cylindrical shell.

The original cylindrical shell laminate has dimensions of length L, thickness h, radius R, and curvature angle β that changes from 30° to 360° in the curvature transformation process. The arc length or "equivalent width" of the cylindrical shell is defined by βR, i.e., (angle) × (radius), which remains constant during the curvature transformation process. Thus, these shells remain about the same overall size. Figure 2 illustrates a piezoelectric laminated cylindrical shell composite.

The four parameters for the cylindrical shell are: Lamé parameters $A_1 = 1$, $A_2 = R$ and radii: $R_1 = \infty$ and $R_2 = R$. Accordingly the electromechanical equations of the cylindrical shell can be derived from those of a generic thick piezoelectric shell laminated composite (Tzou and Bao, 1993).

$$\frac{\partial}{\partial x}(N_{xx}^m - N_{xx}^e) + \frac{1}{R}\frac{\partial}{\partial \theta}(N_{x\theta}^m) = \rho h \ddot{u}_1, \quad (1)$$

$$\frac{\partial}{\partial x}(N_{x\theta}^m) + \frac{1}{R}\frac{\partial}{\partial \theta}(N_{\theta\theta}^m - N_{\theta\theta}^e) + \frac{1}{R}\left[\frac{\partial}{\partial x}(M_{x\theta}^m) + \frac{1}{R}\frac{\partial}{\partial \theta}(M_{\theta\theta}^m - M_{\theta\theta}^e)\right] = \rho h \ddot{u}_2, \quad (2)$$

$$\frac{\partial}{\partial x}\left[\frac{\partial}{\partial x}(M_{xx}^m - M_{xx}^e) + \frac{1}{R}\frac{\partial}{\partial \theta}(M_{x\theta}^m)\right] + \frac{1}{R}\frac{\partial}{\partial \theta}\left[\frac{\partial}{\partial x}(M_{x\theta}^m) + \frac{1}{R}\frac{\partial}{\partial \theta}(M_{\theta\theta}^m - M_{\theta\theta}^e)\right] - \frac{1}{R}(N_{\theta\theta}^m - N_{\theta\theta}^e) = \rho h \ddot{u}_3, \quad (3)$$

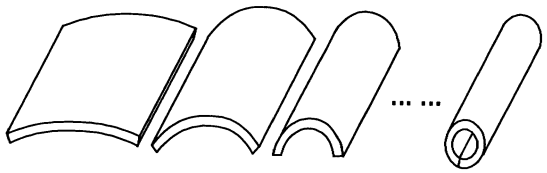

FIGURE 1 Shell transformations.

where N_{ij} are membrane forces; M_{ij} are mechanical bending moments; ρ is the mass density; h is the shell thickness; and u_1, u_2, and u_3 are the displacements in the x, θ, and α_3 directions, respectively. The superscript m denotes the mechanical component and e the electric component. Mechanical forces and moments are related to deflections u_1, u_2, and u_3:

$$N_{xx}^m = A_{11}\left(\frac{\partial u_1}{\partial x}\right) + A_{12}\frac{1}{R}\left(\frac{\partial u_2}{\partial \theta} + u_3\right), \quad (4a)$$

$$N_{\theta\theta}^m = A_{12}\left(\frac{\partial u_1}{\partial x}\right) + A_{22}\frac{1}{R}\left(\frac{\partial u_2}{\partial \theta} + u_3\right), \quad (4b)$$

$$N_{x\theta}^m = A_{66}\left(\frac{1}{R}\frac{\partial u_1}{\partial \theta} + \frac{\partial u_2}{\partial x}\right), \quad (4c)$$

$$M_{xx}^m = D_{11}\left(-\frac{\partial^2 u_3}{\partial x^2}\right) + D_{12}\frac{1}{R^2}\left(\frac{\partial u_2}{\partial \theta} - \frac{\partial^2 u_3}{\partial \theta^2}\right), \quad (4d)$$

$$M_{\theta\theta}^m = D_{12}\left(-\frac{\partial^2 u_3}{\partial x^2}\right) + D_{22}\frac{1}{R^2}\left(\frac{\partial u_2}{\partial \theta} - \frac{\partial^2 u_3}{\partial \theta^2}\right), \quad (4e)$$

$$M_{x\theta}^m = D_{66}\frac{1}{R}\left(\frac{\partial u_2}{\partial x} - 2\frac{\partial^2 u_3}{\partial x \partial \theta}\right), \quad (4f)$$

where A_{ij} and D_{ij} are, respectively, the extensional and bending stiffness (Tzou and Bao,

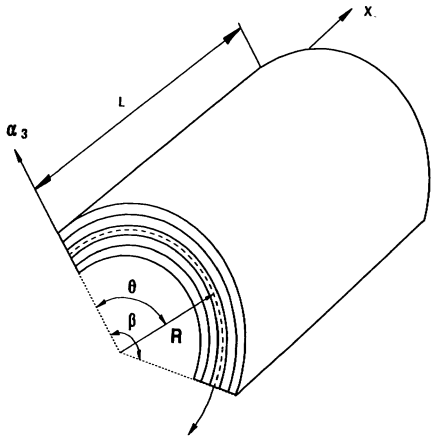

FIGURE 2 A piezoelectric laminated cylindrical shell composite.

1993). For illustration, it is assumed that the cylindrical shell laminated composite is made of five layers: two piezoelectric layers on the top and bottom surfaces and three laminae between these two piezoelectric layers. (A subscript or sub-subscript is used to denote the ith layer in later derivations.) Electric forces and moments are contributed by two components: the converse effect (with a superscript c) and the direct effect (with a superscript d). In practice, the former is related to control voltages and the latter is related to elastic and electric couplings.

$$N^e_{xx} = N^c_{xx} + N^d_{xx} = -e_{31}(\phi^c_{31} + \phi^c_{35}) - \frac{2e^2_{31}}{\varepsilon_{33}}\left[\frac{\partial u_1}{\partial x} + \frac{1}{R}\left(\frac{\partial u_2}{\partial \theta} + u_3\right)\right] h_1, \tag{5a}$$

$$N^e_{\theta\theta} = N^e_{xx}, \quad N^e_{x\theta} = 0, \tag{5b,c}$$

$$M^e_{xx} = M^c_{xx} + M^d_{xx} = -\frac{e_{31}}{2}(\phi^c_{35} - \phi^c_{31})(h_1 + 3h_2) - \frac{2e^2_{31}}{3\varepsilon_{33}}\left[-\frac{\partial^2 u_3}{\partial x^2} + \frac{1}{R^2}\left(\frac{\partial u_2}{\partial \theta} - \frac{\partial^2 u_3}{\partial \theta^2}\right)\right] \cdot \left(h_1^3 + \frac{9}{2}h_1^2 h_2 + \frac{27}{4}h_1 h_2^2\right), \tag{5d}$$

$$M^e_{\theta\theta} = M^e_{xx}, \quad M^e_{x\theta} = 0, \tag{5e,f}$$

where e_{31} is the piezoelectric constant; ϕ^c_{3i} is the transverse electric field applied to the ith layer, ε_{33} is the electric permittivity; h_i is the ith layer thickness. Note that it is assumed that the two piezoelectric layers have the same thickness, i.e., $h_1 = h_5$, and they are, respectively, the first and fifth layer in the laminated composite. The other three layers have the same thickness simply represented by an h_2 in the expressions. Substituting these relations into the composite electromechanical equations yields:

$$\left(A_{11} + \frac{2e^2_{31}h_1}{\varepsilon_{33}}\right)\left(\frac{\partial^2 u_x}{\partial x^2}\right) + \left(A_{12} + \frac{2e^2_{31}h_1}{\varepsilon_{33}}\right)\frac{1}{R}\left(\frac{\partial^2 u_\theta}{\partial\theta\partial x} + \frac{\partial u_3}{\partial x}\right) + \frac{1}{R}A_{66}\left(\frac{1}{R}\frac{\partial^2 u_x}{\partial\theta^2} + \frac{\partial^2 u_\theta}{\partial x\partial\theta}\right) = \rho h\ddot{u}_x, \tag{6}$$

$$A_{66}\left(\frac{1}{R}\frac{\partial^2 u_x}{\partial x\partial\theta} + \frac{\partial^2 u_\theta}{\partial x^2}\right) + \frac{1}{R}\left(A_{12} + \frac{2e^2_{31}h_1}{\varepsilon_{33}}\right)\left(\frac{\partial^2 u_x}{\partial x\partial\theta}\right) + \frac{1}{R^2}\left(A_{22} + \frac{2e^2_{31}h_1}{\varepsilon_{33}}\right)\left(\frac{\partial^2 u_\theta}{\partial\theta^2} + \frac{\partial u_3}{\partial\theta}\right) + D_{66}\frac{1}{R^2}\left(\frac{\partial^2 u_\theta}{\partial x^2} - 2\frac{\partial^3 u_3}{\partial x^2\partial\theta}\right) - \frac{1}{R^2}\left[D_{12} + \frac{2e^2_{31}}{3\varepsilon_{33}}\left(h_1^3 + \frac{9}{2}h_1^2h_2 + \frac{27}{4}h_1h_2^2\right)\right]\frac{\partial^3 u_3}{\partial\theta\partial x^2} + \frac{1}{R^4}\left[D_{22} + \frac{2e^2_{31}}{3\varepsilon_{33}}\left(h_1^3 + \frac{9}{2}h_1^2h_2 + \frac{27}{4}h_1h_2^2\right)\right] \cdot \left(\frac{\partial^2 u_\theta}{\partial\theta^2} - \frac{\partial^3 u_3}{\partial\theta^3}\right) = \rho h\ddot{u}_\theta, \tag{7}$$

$$\left[D_{11} + \frac{2e^2_{31}}{3\varepsilon_{33}}\left(h_1^3 + \frac{9}{2}h_1^2h_2 + \frac{27}{4}h_1h_2^2\right)\right] \cdot \left(-\frac{\partial^4 u_3}{\partial x^4}\right) + \frac{1}{R^2} \cdot \left[D_{12} + \frac{2e^2_{31}}{3\varepsilon_{33}}\left(h_1^3 + \frac{9}{2}h_1^2h_2 + \frac{27}{4}h_1h_2^2\right)\right] \cdot \left(\frac{\partial^3 u_\theta}{\partial\theta\partial x^2} - \frac{\partial^4 u_3}{\partial\theta^2\partial x^2}\right) + D_{66}\frac{2}{R^2}\left(\frac{\partial^3 u_\theta}{\partial\theta\partial x^2} - 2\frac{\partial^4 u_3}{\partial x^2\partial\theta^2}\right) + \frac{1}{R^2}\left[D_{12} + \frac{2e^2_{31}}{3\varepsilon_{33}}\left(h_1^3 + \frac{9}{2}h_1^2h_2 + \frac{27}{4}h_1h_2^2\right)\right] \cdot \left(-\frac{\partial^4 u_3}{\partial x^2\partial\theta^2}\right) + \frac{1}{R^4}\left[D_{22} + \frac{2e^2_{31}}{3\varepsilon_{33}} \cdot \left(h_1^3 + \frac{9}{2}h_1^2h_2 + \frac{27}{4}h_1h_2^2\right)\right]\left(\frac{\partial^3 u_\theta}{\partial\theta^3} - \frac{\partial^4 u_3}{\partial\theta^4}\right) - \frac{e_{31}}{R}(\phi^c_{31} + \phi^c_{35}) - \frac{1}{R}\left(A_{12} + \frac{2e^2_{31}h_1}{\varepsilon_{33}}\right)\left(\frac{\partial u_x}{\partial x}\right) - \left(A_{22} + \frac{2e^2_{31}h_1}{\varepsilon_{33}}\right)\frac{1}{R^2}\left(\frac{\partial u_\theta}{\partial\theta} + u_3\right) = \rho h\ddot{u}_3. \tag{8}$$

Simplifying these equations gives

$$K_1\frac{\partial^2 u_x}{\partial x^2} + K_2\frac{\partial^2 u_\theta}{\partial\theta\partial x} + K_3\frac{\partial^2 u_x}{\partial\theta^2} + K_4\frac{\partial u_3}{\partial x} - \rho h\ddot{u}_x = 0, \tag{9}$$

$$K_5\frac{\partial^2 u_\theta}{\partial x^2} + K_6\frac{\partial^2 u_\theta}{\partial\theta^2} + K_7\frac{\partial^2 u_x}{\partial x\partial\theta} + K_8\frac{\partial^3 u_3}{\partial x^2\partial\theta} + K_9\frac{\partial^3 u_3}{\partial\theta^3} + K_{10}\frac{\partial u_3}{\partial\theta} - \rho h\ddot{u}_\theta = 0, \tag{10}$$

$$K_{11}\frac{\partial^4 u_3}{\partial x^4} + K_{12}\frac{\partial^4 u_3}{\partial\theta^2\partial x^2} + K_{13}\frac{\partial^4 u_3}{\partial\theta^4} + K_{14}\frac{\partial^3 u_\theta}{\partial\theta\partial x^2} + K_{15}\frac{\partial^3 u_\theta}{\partial\theta^3} + K_{16}\frac{\partial u_x}{\partial x} + K_{17}\left(\frac{\partial u_\theta}{\partial\theta} + u_3\right) - \rho h\ddot{u}_3 - \frac{e_{31}}{R}(\phi_{31}^c + \phi_{35}^c) = 0, \tag{11}$$

where the coefficients K_{ij} are defined in the Appendix. Again, the electromechanical equations are valid for the transforming cylindrical shell laminated composite as long as the curvature angles are defined. Natural frequencies and damping ratios of the shells with control voltages applied to the piezoelectric actuators are evaluated next.

FREE VIBRATION ANALYSIS

For a simply supported cylindrical shell laminated composite, boundary conditions (S2 boundary conditions) are defined as

$$u_x(x, 0) = u_x(x, \beta) = 0, \quad u_\theta(0, \theta) = u_\theta(L, \theta) = 0, \tag{12a,b}$$

$$u_3(0, \theta) = u_3(L, \theta) = u_3(x, 0) = u_3(x, \beta) = 0. \tag{12c}$$

Oscillations of the shell at its natural frequency ω_{mn} can be assumed in a harmonic form (Soedel, 1993; Tzou, 1993):

$$u_x = U_x(x, \theta)e^{j\omega t}, \quad u_\theta = U_\theta(x, \theta)e^{j\omega t}, \quad u_3 = U_3(x, \theta)e^{j\omega t}, \tag{13a,b,c}$$

where U_i denotes the mode shape function; ω is the oscillation frequency and $\omega = \omega_{mn}$. Solutions of the cylindrical shell with simply supported (S2) boundary conditions can be assumed as

$$u_x(x, \theta, t) = A_{mn}\cos\frac{m\pi x}{L}\sin\frac{n\pi\theta}{\beta}e^{j\omega t}, \tag{14a}$$

$$u_\theta(x, \theta, t) = B_{mn}\sin\frac{m\pi x}{L}\cos\frac{n\pi\theta}{\beta}e^{j\omega t}, \tag{14b}$$

$$u_3(x, \theta, t) = C_{mn}\sin\frac{m\pi x}{L}\sin\frac{n\pi\theta}{\beta}e^{j\omega t}. \tag{14c}$$

These assumed solutions need to satisfy all boundary conditions. Substituting these assumed solutions into the electromechanical equations and solving for natural frequencies ω_{imn} and mode shapes, one can find

$$\left[\rho h\omega^2 - K_1\left(\frac{m\pi}{L}\right)^2 - K_3\left(\frac{n\pi}{\beta}\right)^2\right]A_{mn} - K_2\frac{m\pi}{L}\frac{n\pi}{\beta}B_{mn} + K_4\frac{m\pi}{L}C_{mn} = 0, \tag{15}$$

$$-K_7\frac{m\pi}{L}\frac{n\pi}{\beta}A_{mn} + \left[\rho h\omega^2 - K_5\left(\frac{m\pi}{L}\right)^2 - K_6\left(\frac{n\pi}{\beta}\right)^2\right]B_{mn} + \left[-K_8\left(\frac{m\pi}{L}\right)^2\left(\frac{n\pi}{\beta}\right) - K_9\left(\frac{n\pi}{\beta}\right)^3 + K_{10}\left(\frac{n\pi}{\beta}\right)\right]C_{mn} = 0, \tag{16}$$

$$-K_{16}\left(\frac{m\pi}{L}\right)A_{mn} + \left[K_{14}\left(\frac{m\pi}{L}\right)^2\left(\frac{n\pi}{\beta}\right) + K_{15}\left(\frac{n\pi}{\beta}\right)^3 - K_{17}\left(\frac{n\pi}{\beta}\right)\right]B_{mn} + \left[\rho h\omega^2 + K_{11}\left(\frac{m\pi}{L}\right)^4 + K_{12}\left(\frac{m\pi}{L}\right)^2\left(\frac{n\pi}{\beta}\right)^2 + K_{13}\left(\frac{n\pi}{\beta}\right)^4 + K_{17}\right]C_{mn} = 0. \tag{17}$$

Note that $K_2 = K_7$, $K_4 = -K_{16}$, $K_8 = -K_{14}$, $K_9 = -K_{15}$, $K_{10} = -K_{17}$. Thus, the eigen equation becomes

$$\begin{bmatrix} \rho h\omega^2 - k_{11} & k_{12} & k_{13} \\ k_{21} & \rho h\omega^2 - k_{22} & k_{23} \\ k_{31} & k_{32} & \rho h\omega^2 - k_{33} \end{bmatrix}\begin{bmatrix} A_{mn} \\ B_{mn} \\ C_{mn} \end{bmatrix} = 0, \tag{18}$$

where

$$k_{11} = K_1\left(\frac{m\pi}{L}\right)^2 + K_3\left(\frac{n\pi}{\beta}\right)^2, \tag{19a,b}$$

$$k_{12} = k_{21} = -K_2\left(\frac{m\pi}{L}\right)\left(\frac{n\pi}{\beta}\right),$$

$$k_{13} = k_{31} = K_4\left(\frac{m\pi}{L}\right), \tag{19c,d}$$

$$k_{22} = K_5\left(\frac{m\pi}{L}\right)^2 + K_6\left(\frac{n\pi}{\beta}\right)^2,$$

$$k_{23} = k_{32} = -K_8\left(\frac{m\pi}{L}\right)^2\left(\frac{n\pi}{\beta}\right) - K_9\left(\frac{n\pi}{\beta}\right)^3 + K_{10}\left(\frac{n\pi}{\beta}\right), \tag{19e}$$

$$k_{33} = -K_{11}\left(\frac{m\pi}{L}\right)^4 - K_{12}\left(\frac{m\pi}{L}\right)^2\left(\frac{n\pi}{\beta}\right)^2 - K_{13}\left(\frac{n\pi}{\beta}\right)^4 - K_{17}. \tag{19f}$$

Taking the determinant of the coefficient matrix zero gives a characteristic equation:

$$\omega^6 + a_1\omega^4 + a_2\omega^2 + a_3 = 0, \tag{20}$$

where coefficients a_i are defined by

$$a_1 = -(k_{11} + k_{22} + k_{33})/\rho h, \tag{21a}$$

$$a_2 = (k_{22}k_{33} + k_{33}k_{11} + k_{11}k_{22} - k_{23}^2 - k_{13}^2 - k_{12}^2)/(\rho h)^2, \tag{21b}$$

$$a_3 = (k_{11}k_{23}^2 + k_{22}k_{13}^2 + k_{33}k_{12}^2 + 2k_{23}k_{13}k_{12} - k_{11}k_{22}k_{33})/(\rho h)^3. \tag{21c}$$

Solving the characteristic equations gives the natural frequencies ω_{1mn}, ω_{2mn}, ω_{3mn}:

$$\omega_{1mn}^2 = -\frac{2}{3}\sqrt{a_1^2 - 3a_2}\cos\frac{\alpha}{3} - \frac{a_1}{3}, \tag{22a}$$

$$\omega_{2mn}^2 = -\frac{2}{3}\sqrt{a_1^2 - 3a_2}\cos\left[\frac{\alpha + 2\pi}{3}\right] - \frac{a_1}{3}, \tag{22b}$$

$$\omega_{3mn}^2 = -\frac{2}{3}\sqrt{a_1^2 - 3a_2}\cos\left[\frac{\alpha + 4\pi}{3}\right] - \frac{a_1}{3}, \tag{22c}$$

and

$$\alpha = \cos^{-1}\left(\frac{27a_3 + 2a_1^3 - 9a_1a_2}{2\sqrt{(a_1^2 - 3a_2)^3}}\right). \tag{22d}$$

Note that for the mnth mode, i.e., every (m, n) combination, there are three *component* natural frequencies. Usually, the lowest frequency is associated with the transverse mode, and the other two frequencies are usually higher by an order of magnitude and they are associated with the in-plane modes, i.e., longitudinal modes and circumferential modes (Tzou, 1993). Accordingly there are three definitions of the modal amplitudes A_{imn}, B_{imn}, and C_{imn} for the mnth mode, each (m, n) combination. Their relative modal amplitude ratios can be obtained from

$$\begin{pmatrix} \rho h\omega_{imn}^2 - k_{11} & k_{12} \\ k_{21} & \rho h\omega_{imn}^2 - k_{22} \end{pmatrix}\begin{pmatrix} A_{imn} \\ B_{imn} \end{pmatrix} = -C_{imn}\begin{pmatrix} k_{13} \\ k_{23} \end{pmatrix}, \quad i = 1, 2, 3, \tag{23}$$

and their normalized modal amplitudes are

$$\begin{pmatrix} A_{imn}/C_{imn} \\ B_{imn}/C_{imn} \end{pmatrix} = -\begin{pmatrix} [k_{13}(\rho h\omega_{imn}^2 - k_{22}) - k_{12}k_{23}]/D_i \\ [k_{23}(\rho h\omega_{imn}^2 - k_{11}) - k_{13}k_{21}]/D_i \end{pmatrix}, \tag{24}$$

where $D_i = (\rho h\omega_{imn}^2 - k_{11})(\rho h\omega_{imn}^2 - k_{22}) - k_{12}^2$. All three u_{ximn}, $u_{\theta imn}$, and u_{3imn} functions together constitute the natural modes (mode shape functions or modal functions)

$$\begin{pmatrix} U_{ximn} \\ U_{\theta imn} \\ U_{3imn} \end{pmatrix} = C_{imn}\begin{pmatrix} \frac{A_{imn}}{C_{imn}}\cos\frac{m\pi x}{L}\cos\frac{n\pi\theta}{\beta} \\ \frac{B_{imn}}{C_{imn}}\sin\frac{m\pi x}{L}\cos\frac{n\pi\theta}{\beta} \\ (1)\ \sin\frac{m\pi x}{L}\cos\frac{n\pi\theta}{\beta} \end{pmatrix}, \tag{25}$$

where the C_{imn} are arbitrary constants. Thus, natural frequencies and mode shapes of the cylindrical shells with different curvatures can be evaluated and compared.

PIEZOELECTRIC CONTROL EFFECTS

The two piezoelectric layers are input with high control voltages, i.e., $\phi_{31}^c = \phi_{35}^c = \phi_3$. It is assumed that the control voltage can be input to infinitesimal "discrete" electrodes, i.e., the voltage is "fully" distributed, and control effectiveness of these cylindrical shells can be evaluated accordingly. In this section, generic displacement, velocity, and acceleration feedback algorithms are formulated, however, the emphasis is placed on the velocity feedback. Because the same voltage is applied to the top and bottom piezoelectric layers: $\phi_{31}^c = \phi_{35}^c = \phi_3$, the last term on the left side of Eq. (11) becomes

$$\frac{e_{31}}{R}(\phi_{31}^c + \phi_{35}^c) = 2\frac{e_{31}}{R}\phi_3. \tag{26}$$

Displacement Feedback

In this case, the control voltage is assumed proportional to the transverse displacement, i.e., $\phi_3 = \mathcal{G}_d u_3$ where $\mathcal{G}_d$ is the displacement control gain. The eigen equation, Eqs. (18), is still the same for the displacement feedback:

$$\begin{pmatrix} \rho h\omega^2 - k_{11} & k_{12} & k_{13} \\ k_{21} & \rho h\omega^2 - k_{22} & k_{23} \\ k_{31} & k_{32} & \rho h\omega^2 - k_{33} \end{pmatrix} \begin{pmatrix} A_{mn} \\ B_{mn} \\ C_{mn} \end{pmatrix} = 0, \tag{27}$$

where the coefficient k_{33} is modified to include the feedback effect:

$$k_{33} = -K_{11}\left(\frac{m\pi}{L}\right)^4 - K_{12}\left(\frac{m\pi}{L}\right)^2\left(\frac{n\pi}{\beta}\right)^2 - K_{13}\left(\frac{n\pi}{\beta}\right)^4 - K_{17} - 2\frac{e_{31}}{R}\mathcal{G}_d. \tag{28}$$

Thus, the characteristic equation can be derived, and frequency and mode shapes with the displacement feedback can be studied.

Velocity Feedback

It is assumed that the control voltage is proportional to the instant transverse velocity, i.e., $\phi_3 = \mathcal{G}_v \dot{u}_3$. The oscillations in three axial directions can be written as

$$u_x(x, \theta, t) = A_{mn}\cos\frac{m\pi x}{L}\sin\frac{n\pi\theta}{\beta}e^{st}, \tag{29a}$$

$$u_\theta(x, \theta, t) = B_{mn}\sin\frac{m\pi x}{L}\cos\frac{n\pi\theta}{\beta}e^{st}, \tag{29b}$$

$$u_3(x, \theta, t) = C_{mn}\sin\frac{m\pi x}{L}\sin\frac{n\pi\theta}{\beta}e^{st}, \tag{29c}$$

where s is a complex frequency. Substituting these assumed solutions into the shell equations gives

$$(-\rho hs^2 - k_{11})A_{mn} + k_{12}B_{mn} + k_{13}C_{mn} = 0, \tag{30a}$$

$$k_{21}A_{mn} + (-\rho hs^2 - k_{22})B_{mn} + k_{23}C_{mn} = 0, \tag{30b}$$

$$k_{31}A_{mn} + k_{32}B_{mn} + \left(-\rho hs^2 - k_{33} - 2\frac{e_{31}}{R}\mathcal{G}_v s\right)C_{mn} = 0, \tag{30c}$$

that is

$$\begin{pmatrix} -\rho hs^2 - k_{11} & k_{12} & k_{13} \\ k_{21} & -\rho hs^2 - k_{22} & k_{23} \\ k_{31} & k_{32} & -\rho hs^2 - k_{33} - 2\frac{e_{31}\mathcal{G}_v}{R}s \end{pmatrix} \begin{pmatrix} A_{mn} \\ B_{mn} \\ C_{mn} \end{pmatrix} = 0. \tag{31}$$

The characteristic equation becomes

$$\begin{aligned} &-(\rho hs^2 + k_{11})(\rho hs^2 + k_{22})\left(\rho hs^2 + k_{33} + 2\frac{e_{31}}{R}\mathcal{G}_v s\right) + 2k_{12}k_{13}k_{23} \\ &+ k_{13}^2(\rho hs^2 + k_{22}) + k_{12}^2\left(\rho hs^2 + k_{33} + 2\frac{e_{31}}{R}\mathcal{G}_v s\right) + k_{23}^2(\rho hs^2 + k_{11}) = 0. \end{aligned} \tag{32}$$

Simply,

$$a_1 s^6 + a_2 s^5 + a_3 s^4 + a_4 s^3 + a_5 s^2 + a_6 s + a_7 = 0, \tag{33}$$

where

$$a_1 = (\rho h)^3, \quad a_2 = 2\frac{e_{31}}{R}\mathcal{G}_v(\rho h)^2, \tag{34a,b}$$

$$a_3 = (k_{11} + k_{22} + k_{33})(\rho h)^2, \tag{34c}$$

$$a_4 = (k_{11} + k_{22})\left(2\frac{e_{31}}{R}\mathcal{G}_v\rho h\right), \tag{34d}$$

$$a_5 = (k_{11}k_{22} + k_{11}k_{33} + k_{22}k_{33} - k_{12}^2 - k_{13}^2 - k_{23}^2)(\rho h), \tag{34e}$$

$$a_6 = (k_{11}k_{22} - k_{12}^2)\left(2\frac{e_{31}}{R}\mathcal{G}_v\right), \tag{34f}$$

$$a_7 = (k_{11}k_{22}k_{33} - 2k_{12}k_{13}k_{23} - k_{11}k_{23}^2 - k_{22}k_{13}^2 - k_{33}k_{12}^2). \tag{34g}$$

The complex frequencies can be calculated as

$$s_{imn} = \mathrm{Re}(s_{imn}) \pm j\mathrm{Im}(s_{imn}), \quad i = 1, 2, 3. \quad (35)$$

Knowing that the complex frequency has the form $s_{imn} = -\zeta_{imn}\omega_{imn} \pm j\omega_{imn}\sqrt{1 - \xi_{imn}^2}$, one can derive

$$\omega_{imn} = |s_{imn}| = \sqrt{\mathrm{Re}(s_{imn})^2 + \mathrm{Im}(s_{imn})^2}, \quad (36a)$$

$$\zeta_{imn} = -\mathrm{Re}(s_{imn})/|s_{imn}|. \quad (36b)$$

Thus, control effects on the frequency and damping variations can be evaluated.

Acceleration Feedback

It is assumed that the control voltage is proportional to the transverse acceleration signal, i.e., $\phi_3 = \mathcal{G}_a\ddot{u}_3$. The eigen equation can be derived as

$$\begin{pmatrix} \rho h\omega^2 - k_{11} & k_{12} & k_{13} \\ k_{21} & \rho h\omega^2 - k_{22} & k_{23} \\ k_{31} & k_{32} & \left(\rho h + 2\dfrac{e_{31}\mathcal{G}_a}{R}\right)\omega^2 - k_{33} \end{pmatrix} \cdot \begin{pmatrix} A_{mn} \\ B_{mn} \\ C_{mn} \end{pmatrix} = 0, \quad (37)$$

and the characteristic equation becomes

$$\omega^6 + a_1\omega^4 + a_2\omega^2 + a_3 = 0, \quad (38)$$

where

$$a_1 = -(k_{11} + k_{22})/\rho h - k_{33}\Big/\left(\rho h + 2\frac{e_{31}\mathcal{G}_a}{R}\right), \quad (39a)$$

$$a_2 = (k_{22}k_{33} + k_{33}k_{11} - k_{23}^2 - k_{13}^2)/(\rho h) \cdot \left(\rho h + 2\frac{e_{31}\mathcal{G}_a}{R}\right) + (k_{11}k_{22} - k_{12}^2)/(\rho h)^2, \quad (39b)$$

$$a_3 = (k_{11}k_{23}^2 + k_{22}k_{13}^2 + k_{33}k_{12}^2 + 2k_{23}k_{13}k_{12} - k_{11}k_{22}k_{33})/(\rho h)^2\left(\rho h + 2\frac{e_{31}\mathcal{G}_a}{R}\right). \quad (39c)$$

Although, three generic feedback control algorithms were derived, the emphasis is placed on the velocity feedback because it is usually more effective than the other two control algorithms in distributed vibration controls (Tzou, 1993).

CASE STUDIES: TRANSFORMATION OF CYLINDRICAL SHELLS

It is assumed that a cylindrical composite shell is transforming from an open shallow shell at $\beta = 30°$, to a deep cylindrical shell at $\beta = 360°$. Note that external forces causing the curvature changes are not considered in the analyses and these shells are evaluated at their static equilibrium positions. It is assumed that a finite separation still exists even when $\beta = 360°$. Recall that the cylindrical shell is (S2) simply supported and the dimensions are: length $L = 10$ cm, $\beta R = 10$ cm, $h = 0.05$ cm $\times$ 5 (layers) $= 0.25$ cm. The initial damping is assumed zero. Figure 2 illustrates the piezoelectric laminated cylindrical shell composite. The transverse mode shapes are determined by $U_3(x, \theta) = \sin(m\pi x/L)\sin(n\pi\theta/\beta)$ in which m denotes the longitudinal half-wave numbers and n the circumferential half-wave numbers. Variations of natural frequencies and controlled damping ratios (via the velocity feedback) are evaluated at every 30° interval ($\beta = i\pi/6$, $i = 1, 2, \ldots, 12$) of curvature changes.

Natural Frequencies

Natural frequencies of the uncontrolled cylindrical shells with different curvatures are calculated and plotted in Fig. 3–5. The vertical axis denotes the natural frequency (Hz) and the horizontal axis denotes the curvature angles β. Figure 3 shows the frequency variations of the ($m = 1$, $n = 1$–5) natural modes, Fig., 4 the ($m = 2$, $n = 1$–5) modes, and Fig. 5 the ($m = 3$, $n = 1$–5) modes. It is observed that for shallow shells the natural frequency increases as the mode number increases. However, the natural frequency decreases for the first few natural modes and increases as the mode number increases when the curvature becomes significant. This is due to the

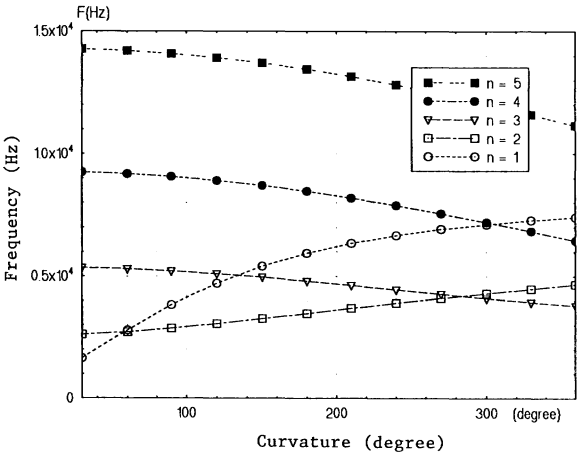

FIGURE 3 Frequency variations of the (m = 1, n = 1–5) modes.

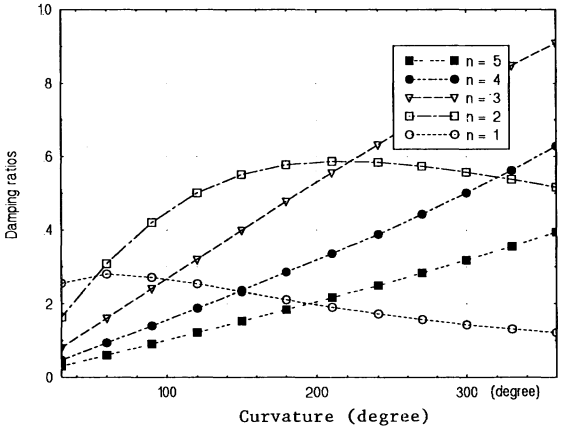

FIGURE 6 Damping ratio variations of the (m = 1, n = 1–5) modes.

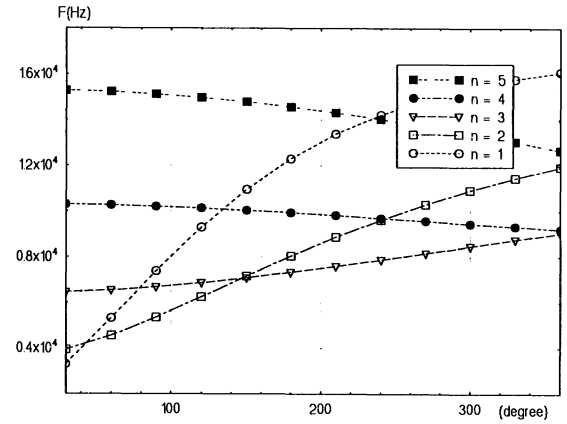

FIGURE 4 Frequency variations of the (m = 2, n = 1–5) modes.

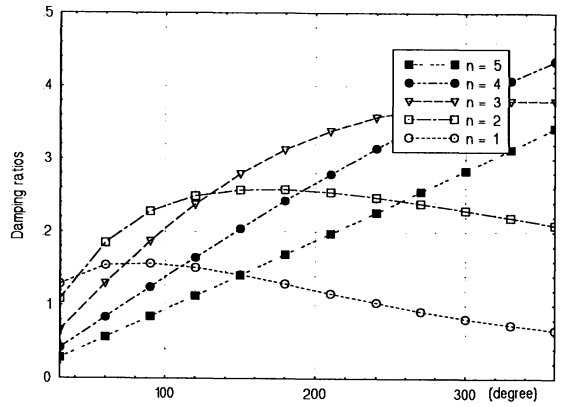

FIGURE 7 Damping ratio variations of the (m = 2, n = 1–5) modes.

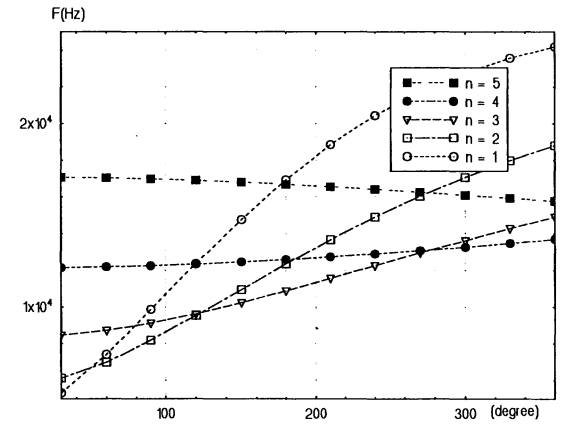

FIGURE 5 Frequency variations of the (m = 3, n = 1–5) modes.

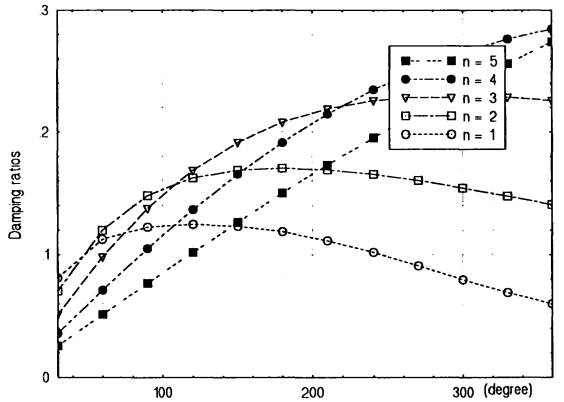

FIGURE 8 Damping ratio variations of the (m = 3, n = 1–5) modes.

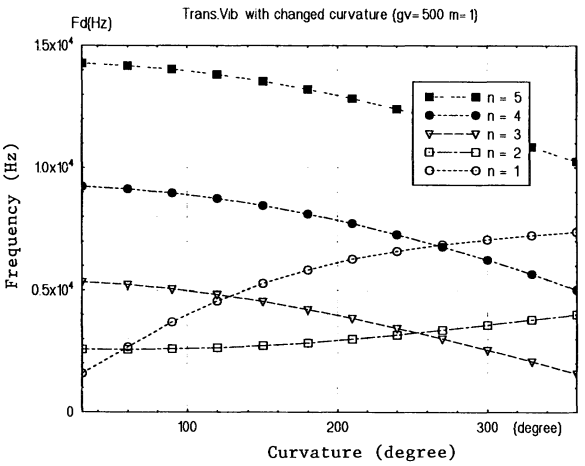

FIGURE 9 Variations of damped natural frequencies, the (m = 1, n = 1–5) modes.

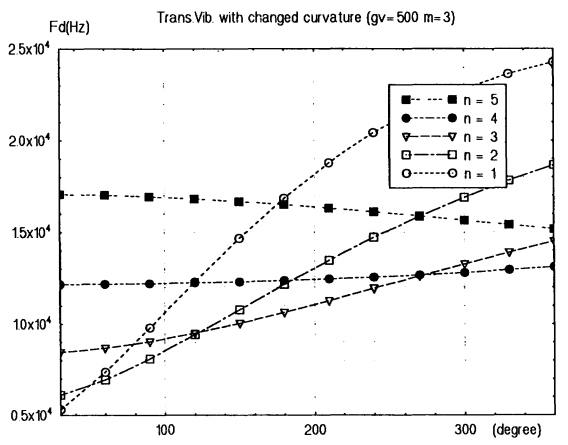

FIGURE 11 Variations of damped natural frequencies, the (m = 3, n = 1–5) modes.

coupling of circumferential and transverse motions in the electromechanical equations. As the curvature increases, this coupling effect increases.

Controlled Damping Ratios

Recall that the initial modal damping ratios are assumed zero, and the damping ratios are introduced by the velocity feedback only. Figures 6–8 illustrate the controlled damping variations of the shells with different curvatures for the (m = 1, n = 1–5), (m = 2, n = 1–5), and (m = 3, n = 1–5) modes when the gain is set at 500. The controlled damping ratio increases as the curvature increases for higher natural modes during the curvature transformation process. However, the damping ratio decreases as the natural frequency increases because there is a natural frequency in the denominator in the damping ratio calculations. These behaviors can be observed in the (m = 1, n = 1, 2) modes, (m = 2, n = 1–3), etc. modes. Damping variations of the transformation shells for the (m = 1, n = 1–5), (m = 2, n = 1–5), and (m = 3, n = 1–5) modes when the gain is set at 1,000 are also studied and their results basically lead to similar conclusions.

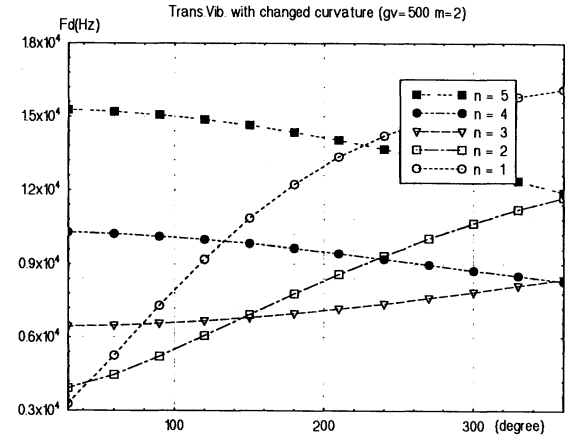

FIGURE 10 Variations of damped natural frequencies, the (m = 2, n = 1–5) modes.

Damped Natural Frequencies

Based on the controlled damping ratios, one can further calculate damped natural frequencies for the cylindrical shell with different curvatures. Figures 9–11 give the variations of damped natural frequencies for the the (m = 1, n = 1–5), (m = 2, n = 1–5), and (m = 3, n = 1–5) modes over the range of curvature transformation when the gain is set at 500. It can be observed that the control effects to the lower modes are more significant than the higher modes.

CONCLUSIONS

Adaptive structures with controllable geometries and shapes offer many advantages over conventional fixed-geometry structures. In this study dynamics and control effectiveness of an adaptive cylindrical shell laminated composite, which transforms from an open shallow shell (30°) to a

deep cylindrical shell (360°), were investigated. A mathematical model for the piezoelectric laminated cylindrical shell composite was formulated and natural frequencies and mode shapes were analyzed. These generic equations and solutions included a curvature angle that can be easily changed to accommodate the curvature transformations. Three generic feedback controls were proposed and the velocity feedback was used in a case study. Control force level was determined by actuator material properties and also control voltages. Numerical analyses of the transforming cylindrical shell suggested the following.

1. Controlled damping ratio of the cylindrical shell decreases as the shell curvature increases for lower natural modes. However, controlled damping ratio keeps increasing for higher natural modes.
2. Natural frequencies of lower natural modes increase and those of higher modes decrease in the process of curvature transformation from 30° to 360°. When the shell curvature increases, dynamic coupling between the circumferential and transverse modes becomes significant. Accordingly, the lowest mode is usually not the first mode for high-curvature shells.

Note that the shell dynamics and control were evaluated at (deformed) static equilibrium positions after the curvature transformation such that external actuation forces imposing the curvature change are not considered. The external actuation force retained in the transformed shell can significantly affect the stability of the transformed shell if considered. In addition, dynamics and control were evaluated in the linear range (small oscillation); large deformation and geometrical nonlinearity were not considered. These stability and nonlinear effects will be considered in future studies.

APPENDIX

Coefficients in the electromechanical equations of the 5-layer laminated composite cylindrical shell are defined as follows.

$$K_1 = \left(\frac{2Y_p}{1-\mu_p^2}\right)h_1 + \left(\frac{2Y_{2c}-Y_{1c}}{1-\mu_{12c}\mu_{21c}}\right)h_2 + \frac{2e_{31}^2 h_1}{\varepsilon_{33}}, \tag{A.1}$$

$$K_2 = \frac{1}{R}\left[\left(\frac{2Y_p\mu_p}{1-\mu_p^2}\right)h_1 + \left(\frac{3Y_{1c}\mu_{21c}}{1-\mu_{12c}\mu_{21c}}\right)h_2 + \frac{2e_{31}^2 h_1}{\varepsilon_{33}}\right] + \frac{1}{R}(2G_{12p}h_1 + 3G_{12c}h_2), \tag{A.2}$$

$$K_3 = \frac{1}{R^2}(2G_{12p}h_1 + 3G_{12c}h_2), \tag{A.3}$$

$$K_4 = \frac{1}{R}\left[\left(\frac{2Y_p\mu_p}{1-\mu_p^2}\right)h_1 + \left(\frac{3Y_{1c}\mu_{21c}}{1-\mu_{12c}\mu_{21c}}\right)h_2 + \frac{2e_{31}^2 h_1}{\varepsilon_{33}}\right], \tag{A.4}$$

$$K_5 = (2G_{12p}h_1 + 3G_{12c}h_2) + \frac{1}{R^2}\left[\frac{1}{6}G_{12p}(4h_1^3 + 18h_1^2h_2 + 27h_1h_2^2) + \frac{27}{12}G_{12c}h_2^3\right], \tag{A.5}$$

$$K_6 = \frac{1}{R^2}\left[\left(\frac{2Y_p}{1-\mu_p^2}\right)h_1 + \left(\frac{2Y_{1c}+Y_{2c}}{1-\mu_{12c}\mu_{21c}}\right)h_2 + \frac{2e_{31}^2 h_1}{\varepsilon_{33}}\right] + \frac{1}{R^4}\left[\frac{Y_p}{6(1-\mu_p^2)}(4h_1^3 + 18h_1^2h_2 + 27h_1h_2^2)\right.$$
$$\left. + \left(\frac{26Y_{1c}+Y_{2c}}{12(1-\mu_{12c}\mu_{21c})}\right)h_2^3 + \frac{2e_{31}^2}{3\varepsilon_{33}}\left(h_1^3 + \frac{9}{2}h_1^2h_2 + \frac{27}{4}h_1h_2^2\right)\right], \tag{A.6}$$

$$K_7 = \frac{1}{R}(2G_{12p}h_1 + 3G_{12c}h_2) + \frac{1}{R}\left[\left(\frac{2Y_p\mu_p}{1-\mu_p^2}\right)h_1 + \left(\frac{3Y_{1c}\mu_{21c}}{1-\mu_{12c}\mu_{21c}}\right)h_2 + \frac{2e_{31}^2 h_1}{\varepsilon_{33}}\right], \tag{A.7}$$

$$K_8 = -\frac{2}{R^2}\left[\frac{1}{6}G_{12p}(4h_1^3 + 18h_1^2h_2 + 27h_1h_2^2) + \frac{27}{12}G_{12c}h_2^3\right]$$
$$-\frac{1}{R^2}\left[\frac{Y_p\mu_p}{6(1-\mu_p^2)}\right)(4h_1^3 + 18h_1^2h_2 + 27h_1h_2^2) + \left(\frac{27Y_{1c}\mu_{21c}}{12(1-\mu_{12c}\mu_{21c})}\right)h_2^3$$

$$+\frac{2e_{31}^2}{3\varepsilon_{33}}\left(h_1^3+\frac{9}{2}h_1^2h_2+\frac{27}{4}h_1h_2^2\right)\Bigg], \tag{A.8}$$

$$K_9=-\frac{1}{R^4}\left[\frac{Y_p}{6(1-\mu_p^2)}(4h_1^3+18h_1^2h_2+27h_1h_2^2)+\left(\frac{26Y_{1c}+Y_{2c}}{12(1-\mu_{12c}\mu_{21c})}\right)h_2^3\right.$$
$$\left.+\frac{2e_{31}^2}{3\varepsilon_{33}}\left(h_1^3+\frac{9}{2}h_1^2h_2+\frac{27}{4}h_1h_2^2\right)\right], \tag{A.9}$$

$$K_{10}=\frac{1}{R^2}\left[\left(\frac{2Y_p}{1-\mu_p^2}\right)h_1+\left(\frac{2Y_{1c}+Y_{2c}}{1-\mu_{12c}\mu_{21c}}\right)h_2+\frac{2e_{31}^2h_1}{\varepsilon_{33}}\right], \tag{A.10}$$

$$K_{11}=-\left[\frac{Y_p}{6(1-\mu_p^2)}(4h_1^3+18h_1^2h_2+27h_1h_2^2)+\left(\frac{26Y_{2c}+Y_{1c}}{12(1-\mu_{12c}\mu_{21c})}\right)h_2^3\right.$$
$$\left.+\frac{2e_{31}^2}{3\varepsilon_{33}}\left(h_1^3+\frac{9}{2}h_1^2h_2+\frac{27}{4}h_1h_2^2\right)\right], \tag{A.11}$$

$$K_{12}=-\frac{2}{R^2}\left[\frac{Y_p\mu_p}{6(1-\mu_p^2)}(4h_1^3+18h_1^2h_2+27h_1h_2^2)+\left(\frac{27Y_{1c}\mu_{21c}}{12(1-\mu_{12c}\mu_{21c})}\right)h_2^3\right.$$
$$\left.+\frac{2e_{31}^2}{3\varepsilon_{33}}\left(h_1^3+\frac{9}{2}h_1^2h_2+\frac{27}{4}h_1h_2^2\right)\right]$$
$$-\frac{4}{R^2}\left[\frac{1}{6}G_{12p}(4h_1^3+18h_1^2h_2+27h_1h_2^2)+\frac{27}{12}G_{12c}h_2^3\right], \tag{A.12}$$

$$K_{13}=-\frac{1}{R^4}\left[\frac{Y_p}{6(1-\mu_p^2)}(4h_1^3+18h_1^2h_2+27h_1h_2^2)+\left(\frac{26Y_{1c}+Y_{2c}}{12(1-\mu_{12c}\mu_{21c})}\right)h_2^3\right.$$
$$\left.+\frac{2e_{31}^2}{3\varepsilon_{33}}\left(h_1^3+\frac{9}{2}h_1^2h_2+\frac{27}{4}h_1h_2^2\right)\right], \tag{A.13}$$

$$K_{14}=\frac{1}{R^2}\left[\frac{Y_p\mu_p}{6(1-\mu_p^2)}(4h_1^3+18h_1^2h_2+27h_1h_2^2)+\left(\frac{27Y_{1c}\mu_{21c}}{12(1-\mu_{12c}\mu_{21c})}\right)h_2^3\right.$$
$$\left.+\frac{2e_{31}^2}{3\varepsilon_{33}}\left(h_1^3+\frac{9}{2}h_1^2h_2+\frac{27}{4}h_1h_2^2\right)\right]$$
$$+\frac{2}{R^2}\left[\frac{1}{6}G_{12p}(4h_1^3+18h_1^2h_2+27h_1h_2^2)+\frac{27}{12}G_{12c}h_2^3\right], \tag{A.14}$$

$$K_{15}=\frac{1}{R^4}\left[\frac{Y_p}{6(1-\mu_p^2)}(4h_1^3+18h_1^2h_2+27h_1h_2^2)+\left(\frac{26Y_{1c}+Y_{2c}}{12(1-\mu_{12c}\mu_{21c})}\right)h_2^3\right.$$
$$\left.+\frac{2e_{31}^2}{3\varepsilon_{33}}\left(h_1^3+\frac{9}{2}h_1^2h_2+\frac{27}{4}h_1h_2^2\right)\right], \tag{A.15}$$

$$K_{16}=-\frac{1}{R}\left[\left(\frac{2Y_p\mu_p}{1-\mu_p^2}\right)h_1+\left(\frac{3Y_{1c}\mu_{21c}}{1-\mu_{12c}\mu_{21c}}\right)h_2+\frac{2e_{31}^2h_1}{\varepsilon_{33}}\right], \tag{A.16}$$

$$K_{17}=-\frac{1}{R^2}\left[\left(\frac{2Y_p}{1-\mu_p^2}\right)h_1+\left(\frac{2Y_{1c}+Y_{2c}}{1-\mu_{12c}\mu_{21c}}\right)h_2+\frac{2e_{31}^2h_1}{\varepsilon_{33}}\right], \tag{A.17}$$

where Y_x is Young's modulus of material x; μ_x is Poisson's ratio of material x; G_{ij} is the shear modulus; the subscript p denotes the piezoelectric material; and the subscript c denotes that elastic composite lamina.

This study was supported by a research grant from the Army Research Office (DAAL-3-91-G0065)(1991–1994). The technical monitor, Dr. G. L. Anderson, is gratefully acknowledged.

REFERENCES

Miura, K., and Furuya, H., 1988, "An Adaptive Structure Concept for Future Space Applications," *AIAA Journal,* Vol. 26, pp. 995–1093.

Natori, M. C., Iwasaki, K., and Kuwao, F., 1987, "Adaptive Planar Truss Structures and Their Vibration Characteristics," AIAA-87-0743, Part 2A, pp. 143–151, *28th SDM Conference,* Monterey, CA, April.

Paul, R. P., 1981, *Robot Manipulators, Mathematics, Programming, and Control,* MIT Press, Cambridge, MA.

Soedel, W., 1993, *Vibrations of Shells and Plates,* Dekker, New York.

Tzou, H. S., 1993, *Piezoelectric Shells (Distributed Sensing and Control of Continua),* Kluwer Academic Publishers, Dordrecht/Boston/London.

Tzou, H. S., and Bao, Y., 1994, "Modeling of Thick Composite Piezoelectric Shell Transducers Laminates," *Journal of Smart Materials and Structures,* Vol. 3, pp. 285–292.

Wada, B. K., Fanson, J. L., and Crawley, E. F., 1989, "Adaptive Structures," *Adaptive Structures,* AD-Vol. 15, pp. 1–8, 1989 ASME Winter Annual Meetings, San Francisco, CA, Dec. 1–5, 1989.